

# Characterization of Lignin Structures and Lignin–Carbohydrate Complex (LCC) Linkages by Quantitative $^{13}\text{C}$ and 2D HSQC NMR Spectroscopy

Tong-Qi Yuan,<sup>†</sup> Shao-Ni Sun,<sup>†</sup> Feng Xu,<sup>\*,†</sup> and Run-Cang Sun<sup>\*,†,‡</sup>

<sup>†</sup>Institute of Biomass Chemistry and Technology, Beijing Forestry University, Beijing, China

<sup>‡</sup>State Key Laboratory of Pulp and Paper Engineering, South China University of Technology, Guangzhou, China

**ABSTRACT:** To characterize the lignin structures and lignin–carbohydrate complex (LCC) linkages, milled wood lignin (MWL) and mild acidolysis lignin (MAL) with a high content of associated carbohydrates were sequentially isolated from ball-milled poplar wood. Quantification of their structural features has been achieved by using a combination of quantitative  $^{13}\text{C}$  and 2D HSQC NMR techniques. The results showed that acetylated 4-*O*-methylglucoxyylan is the main carbohydrate associated with lignins, and acetyl groups frequently acylate the C2 and C3 positions. MWL and MAL exhibited similar structural features. The main substructures were  $\beta$ -*O*-4' aryl ether, resinol, and phenylcoumaran, and their abundances per 100 Ar units changed from 41.5 to 43.3, from 14.6 to 12.7, and from 3.7 to 4.0, respectively. The S/G ratios were estimated to be 1.57 and 1.62 for MWL and MAL, respectively. Phenyl glycoside and benzyl ether LCC linkages were clearly quantified, whereas the amount of  $\gamma$ -ester LCC linkages was ambiguous for quantification.

**KEYWORDS:** milled wood lignin, mild acidolysis lignin, lignin–carbohydrate complex, poplar, quantitative  $^{13}\text{C}$  NMR, HSQC, quantification

## INTRODUCTION

Lignin is an aromatic heteropolymer and the second most abundant plant biopolymer after cellulose. Generally, it is considered as being formed by the dehydrogenative polymerization of three hydroxycinnamyl alcohols: *p*-coumaryl, coniferyl, and sinapyl alcohols.<sup>1–3</sup> Each of these monolignols gives rise to different types of lignin units called *p*-hydroxyphenyl (H), guaiacyl (G), and syringyl (S) units, respectively. Lignin is deposited mostly in the secondary cell walls of vascular plants and is essential for water transport, mechanical support, and plant pathogen defense.<sup>4</sup> As a major component of plant cell walls, lignin has long been studied in the area of papermaking as well as biofuel production in recent years.<sup>5,6</sup>

Although the complex and irregular structure of lignin has been extensively investigated, it has not yet been completely elucidated.<sup>2,3</sup> Two major obstacles in the elucidation of the structure of native lignin could be summarized. The primary one is that it cannot be isolated in a chemically unaltered form because of the tight physical binding and chemical linkages between lignin and cell wall polysaccharides.<sup>7</sup> The major inter-unit linkages within the lignin macromolecules are  $\beta$ -*O*-4',  $\beta$ - $\beta$ ',  $\beta$ -5',  $\beta$ -1', etc.,<sup>8</sup> whereas the main types of lignin–carbohydrate complex (LCC) linkages in wood are believed to be phenyl glycoside bonds, esters, and benzyl ethers.<sup>8–11</sup> The other obstacle is the lack of ideal techniques, which could provide adequate and quantitative information for the entire lignin structure and various LCC linkages.<sup>11–17</sup>

In the past several decades various methods have been developed to isolate lignin from plant cell walls. The first major method was proposed by Björkman,<sup>18</sup> who extracted lignin from finely ball-milled wood with aqueous dioxane. The milled wood

lignin (MWL) obtained is considered to be a representative source of native lignin and has been extensively used in the elucidation of native lignin structure. However, the yield of MWL is limited and heavily dependent upon milling time.<sup>19</sup> To improve yield while minimizing the extent of mechanical action, the method to isolate cellulolytic enzyme lignin (CEL) was proposed by Pew.<sup>20</sup> Some improved methods to isolate CEL were subsequently brought forward.<sup>21–23</sup> CEL was found to be structurally similar to MWL,<sup>14,20,21</sup> but in a higher yield, and hence it is more representative of the total lignin in wood than MWL. Recently, a novel procedure using the combination of enzymatic and mild acidolysis was proposed, and the obtained lignin preparation was named enzymatic mild acidolysis lignin (EMAL).<sup>24</sup> It has been reported that EMAL is more representative of the total lignin present in milled wood and offers higher yields and purities than those of the corresponding MWL and CEL.<sup>25</sup> Besides, EMAL is released by cleaving lignin–carbohydrate bonds rather than other linkages within the lignin macromolecules.<sup>24,25</sup>

Most of the information on lignin and LCC structures was obtained from different wet chemistry techniques and model compound experiments.<sup>26–33</sup> Although information obtained from these methods is very valuable, each gives limited information and is not able to provide a general picture of the entire lignin and LCC structures, particularly if a degradative technique is used.<sup>11,15,16</sup> Various spectroscopic methods have been applied

**Received:** August 6, 2011

**Revised:** August 29, 2011

**Accepted:** September 1, 2011

**Published:** September 01, 2011

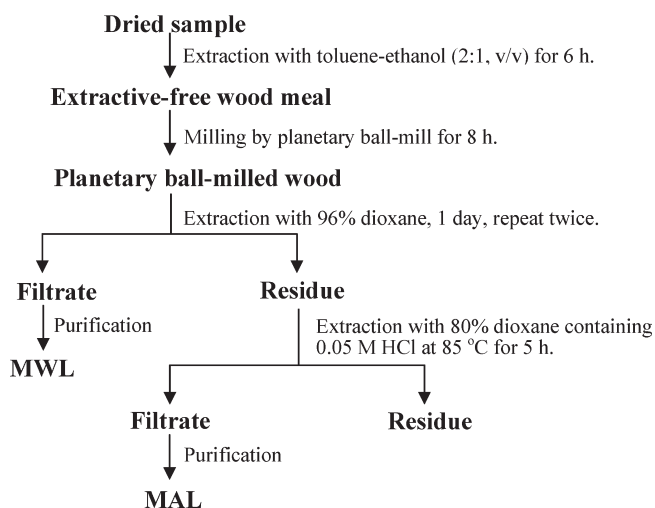


**Figure 1.** Preparation of milled wood lignin (MWL) and mild acidolysis lignin (MAL).

to analyze the whole lignin and LCC structures, such as infrared (IR), solid-state NMR, and solution-state NMR. Among these methods, solution-state NMR has a much higher resolution, which enables a larger amount of information to be obtained.<sup>15</sup>

Especially, quantitative <sup>13</sup>C NMR and two-dimensional heteronuclear single-quantum coherence (2D HSQC) have been developed to quantify the lignin structures and identify the various LCC linkages, respectively.<sup>10,15</sup> However, when the lignin preparation is rich in associated carbohydrates, the quantification of lignin structure and LCC linkages with quantitative <sup>13</sup>C NMR is not so efficient. As the carbohydrate overlap in the side-chain region of the <sup>13</sup>C NMR spectrum can compromise the integration and subsequent quantification of the lignin structures, the 2D NMR method has been used to cope with the overlapping obstacle and attempts have been made to quantify the obtained HSQC spectrum.<sup>34–36</sup> However, the method based on 2D NMR could provide the relative proportions of the detected structures rather than the absolute values. Recently, a new quantification method with the combination of quantitative <sup>13</sup>C and 2D HSQC NMR was proposed by Zhang and Gellerstedt.<sup>17</sup> This approach was verified on cellulose triacetate and MWL, as well as various LCC preparations.<sup>11,17</sup>

In the present study, two lignin preparations with high contents of carbohydrates were isolated from triploid of *Populus tomentosa* Carr., a fast-growing poplar tree. The aim of this study was to identify and quantify the lignin structures and LCC linkages by combining the use of quantitative <sup>13</sup>C and 2D HSQC NMR spectroscopy.

## MATERIALS AND METHODS

**Materials.** Wood sawdust was prepared from triploid of *P. tomentosa* Carr., a fast-growing poplar tree, 3 years old, which was harvested from Shandong province, China. It was extracted with toluene/ethanol (2:1, v/v) in a Soxhlet instrument for 6 h. The Klason lignin content was measured by the TAPPI standard, which amounts to 20.3% of the dry wood. The extracted sawdust (25 g) was then milled using a planetary ball mill (Fritsch, Germany) in a 500 mL ZrO<sub>2</sub> bowl with mixed balls (10 balls of 2 cm diameter and 25 balls of 1 cm diameter). The milling was conducted for 8 h under a nitrogen atmosphere at 500 rpm. A 10 min pause was introduced after every 10 min of milling to prevent

overheating. All chemicals used were of analytical or reagent grade and directly used as purchased without further purification.

**Isolation of Lignins.** MWL and mild acidolysis lignin (MAL) were isolated according to Figure 1. MWL was isolated according to the method of Björkman.<sup>18</sup> The procedures are as follows: The ball-milled wood sample was suspended in 96% dioxane with a solid-to-liquid ratio of 1:10 (g/mL) at room temperature for 24 h. The extraction procedure was conducted in the dark and under a nitrogen atmosphere. The mixture was filtered and washed with the same solvents until the filtrate was clear. Such operations were repeated twice. The purification procedure was according to the method of Sun et al.<sup>37</sup> The combined filtrates were first concentrated at reduced pressure and then precipitated in 3 volumes of 95% ethanol. A pellet rich in hemicelluloses was recovered by filtering, washing with 70% ethanol, and freeze-drying. After evaporation of ethanol, the 96% dioxane soluble lignin (MWL) was obtained by precipitation at pH 1.5–2.0, which was adjusted by 6 M HCl. MAL was isolated by successively treating the residual wood meal after extraction of MWL with 80% dioxane containing 0.05 M HCl at 85 °C for 5 h. The solid-to-liquid ratio was 1:20 (g/mL). MAL was obtained according to the same method as precipitation of MWL except for washing with acidified water (pH 2.0) before freeze-drying.

**Characterization of Lignins.** The analysis of the carbohydrate moieties associated with MWL and MAL was determined by hydrolysis with dilute sulfuric acid according to the procedure described in a previous paper.<sup>38</sup> The weight-average ( $M_w$ ) and number-average ( $M_n$ ) molecular weights of the two lignin preparations were determined by gel permeation chromatography (GPC) on a PL-gel 10 mm Mixed-B 7.5 mm i.d. column according to a previous paper.<sup>39</sup>

All NMR spectra were recorded on a Bruker AVIII 400 MHz spectrometer at 25 °C in DMSO-*d*<sub>6</sub> as the solvent. For the quantitative <sup>13</sup>C NMR, 125 mg of lignin was dissolved in 0.5 mL of DMSO-*d*<sub>6</sub>. The quantitative <sup>13</sup>C NMR spectra were recorded in the FT mode at 100.6 MHz. The inverse gated decoupling sequence, which allows quantitative analysis and comparison of signal intensities, was used with the following parameters: 30° pulse angle; 1.4 s acquisition time; 2 s relaxation delay; 64K data points; and 30000 scans. Chromium(III) acetylacetonate (0.01 M) was added to the lignin solution to provide complete relaxation of all nuclei.<sup>13</sup>

For the 2D HSQC NMR, around 90 mg of lignin was dissolved in 0.5 mL of DMSO-*d*<sub>6</sub>. 2D HSQC NMR spectra were recorded in HSQC experiments. The spectral widths were 5000 and 20000 Hz for the <sup>1</sup>H and <sup>13</sup>C dimensions, respectively. The number of collected complex points was 1024 for the <sup>1</sup>H dimension with a recycle delay of 1.5 s. The number of transients was 64, and 256 time increments were always recorded in the <sup>13</sup>C dimension. The  $J_{CH}$  used was 145 Hz. Prior to Fourier transformation, the data matrices were zero filled to 1024 points in the <sup>13</sup>C dimension. Data processing was performed using standard Bruker Topspin-NMR software. The central solvent (DMSO) peak was used as an internal chemical shift reference point ( $\delta_C/\delta_H$  39.5/2.49).

## RESULTS AND DISCUSSION

**Lignin Yield and Purity.** The yields and carbohydrate contents of MWL and MAL isolated from triploid of *P. tomentosa* Carr. are given in Table 1. The yield of MWL was 22.1%, which was much higher than the value in a previous study (just 5.4%).<sup>40</sup> This result showed that lignin in the middle layer of the secondary wall (S<sub>2</sub>), which has more linkages with carbohydrates, become extractable as MWL after the carbohydrates were degraded sufficiently under the milling conditions employed. The yield of MAL, which was isolated by successive treatment of the residual wood meal after extraction of MWL with 80% dioxane containing 0.05 M HCl at 85 °C for 5 h, was 52.1%.

**Table 1. Yields and Carbohydrate Contents of Lignin Fractions**

sample	yield (%)			carbohydrate content <sup>a</sup> (%)						
	with sugars <sup>b</sup>	without sugars	total sugar content (%)	Rha	Ara	Gal	Glc	Man	Xyl	Uro
MWL	22.1	18.7	15.40	0.13	0.07	0.32	0.52	nd <sup>c</sup>	13.92	0.47
MAL	52.1	46.7	10.40	0.13	0.03	0.12	0.27	nd	9.24	0.65

<sup>a</sup>Rha, rhamnose; Ara, arabinose; Gal, galactose; Glc, glucose; Man, mannose; Xyl, xylose; Uro, uronic acid <sup>b</sup>Based on Klason lignin of wood. <sup>c</sup>Not detected.

It was believed that a mild acid hydrolysis can cleave the remaining lignin–carbohydrate bonds and liberate lignin from lignin–carbohydrate complexes.<sup>24,25,41</sup>

Generally, to remove the contaminations (associated carbohydrates) within the obtained lignin preparation, tedious purification steps are needed.<sup>18–21</sup> During those procedures, some LCC-rich lignin fractions are lost. In the present study, to obtain lignin preparations with high carbohydrate contents for LCC linkages analysis, the two lignin fractions were purified according to the method of Sun et al.<sup>37</sup> as mentioned above. As can be seen from Table 1, both MWL and MAL contained relatively high levels of associated carbohydrates, amounting to 15.4 and 10.4%, respectively. Obviously, both MWL and MAL contained a larger percentage of xylose (88.8–90.4%) among the total sugars and uronic acids. Other sugars, such as glucose, galactose, and rhamnose, as well as arabinose, were observed in noticeable amounts. It could be noted that some LCC linkages survived the mild acid hydrolysis procedure. This was quite different from a previous study, in which the carbohydrate content in EMAL obtained from poplar wood was just 4.3%.<sup>24</sup> This could be explained by the different isolation methods used. In the previous study, cellulase was used to remove most of the polysaccharides before mild acid hydrolysis. It has been found that  $\beta$ -glycosidases, present in cellulases preparations, can cleave the phenyl glycoside linkages.<sup>31,42,43</sup> Besides, the temperature in the mild acid hydrolysis procedure was lower than used in the previous study.<sup>24</sup> All of these associated carbohydrates will be discussed in detail in the following 2D HSQC spectra analysis.

After calibration of the amounts of associated carbohydrates, the pure yields of MWL and MAL were 18.7 and 46.7%, respectively, as shown in Table 1. The combined yield of MWL and MAL, without cellulolytic enzymatic treatment, was 65.4%, which was close to the yield of EMAL in the previous study.<sup>24</sup> Direct elucidation of the chemical structure of lignin in residual wood meal left after extraction of MWL could be important for understanding the structure of a greater proportion of lignin in the cell wall.<sup>44</sup> If these two preparations are indeed similar, they could be combined to increase the overall yield of pure lignin material.

**Molecular Weight Distributions.** The values of the weight-average ( $M_w$ ) and number-average ( $M_n$ ) molecular weights, calculated from the GPC curves (relative values related to polystyrene), and the polydispersity ( $M_w/M_n$ ) of MWL and MAL are given in Table 2. As can be seen, MWL and MAL exhibited similar weight-average molecular weights, 4710 and 3670 g mol<sup>-1</sup>, respectively. Especially, the weight-average molecular weight of MAL was identical with the value of CEL in our previous study.<sup>40</sup> These data indicated that MAL was released by cleaving lignin–carbohydrate bonds rather than other linkages within the lignin macromolecules in the present study.

**Table 2. Weight-Average ( $M_w$ ) and Number-Average ( $M_n$ ) Molecular Weights and Polydispersity ( $M_w/M_n$ ) of Lignin Fractions**

	MWL	MAL
$M_w$	4710	3670
$M_n$	2730	2060
$M_w/M_n$	1.73	1.78

The weight-average molecular weight of MWL was slightly higher than that of MAL. This phenomenon might be explained by the different contents of carbohydrates associated with these two lignin fractions. It has been documented that the carbohydrate chains linked to lignin can increase the hydrodynamic volume of lignin and therefore increase the apparent molar mass of the lignin when it was measured using GPC.<sup>45</sup> This was in line with the results of carbohydrate analysis as shown in Table 1. Besides, both MWL and MAL exhibited relatively narrow molecular weight distributions, as shown by  $M_w/M_n < 1.80$ .

**2D NMR of MWL and MAL.** Two-dimensional <sup>1</sup>H–<sup>13</sup>C NMR (2D NMR) has been able to provide important structural information and has allowed for the resolution of otherwise overlapping resonances observed in either the <sup>1</sup>H or <sup>13</sup>C NMR spectra.<sup>46</sup> In the present study, to understand the detailed structures of MWL and MAL, as well as the linkages between lignin and the associated carbohydrates, the two lignin fractions were characterized by 2D HSQC NMR techniques. The side-chain ( $\delta_C/\delta_H$  50–90/2.5–6.0) and the aromatic ( $\delta_C/\delta_H$  100–135/5.5–8.5) regions of the HSQC spectra of MWL and MAL are shown in Figure 2. The main substructures are depicted in Figure 3. The well-resolved anomeric correlations ( $\delta_C/\delta_H$  90–105/3.9–5.4) of the associated carbohydrates are shown in Figure 4. HSQC cross-signals of lignin and the associated carbohydrates were assigned by comparison with the published literature.<sup>10,11,35,40,46–54</sup> The main lignin cross-signals assigned in the HSQC spectra are listed in Table 3, whereas the assignments of the associated carbohydrate cross-signals are listed in Table 4.

**Lignin Side-Chain Regions.** The side-chain region ( $\delta_C/\delta_H$  50–90/2.5–6.0) of the 2D HSQC NMR spectra provided useful information about the interunit linkages present in lignin. As shown in Figure 2 (left column), the side-chain regions of MWL and MAL in the HSQC spectra were similar. Both spectra showed prominent signals corresponding to methoxyls ( $\delta_C/\delta_H$  55.6/3.73) and  $\beta$ -O-4' aryl ether linkages. The  $C_\alpha$ – $H_\alpha$  correlations in  $\beta$ -O-4' substructures were observed at  $\delta_C/\delta_H$  71.8/4.86 (structures A and A'), whereas the  $C_\beta$ – $H_\beta$  correlations corresponding to the *erythro* and *threo* forms of the S-type  $\beta$ -O-4' substructures can be distinguished at  $\delta_C/\delta_H$  85.9/4.12 and 86.8/3.99, respectively. These correlations shifted to  $\delta_C/\delta_H$  83.9/4.29

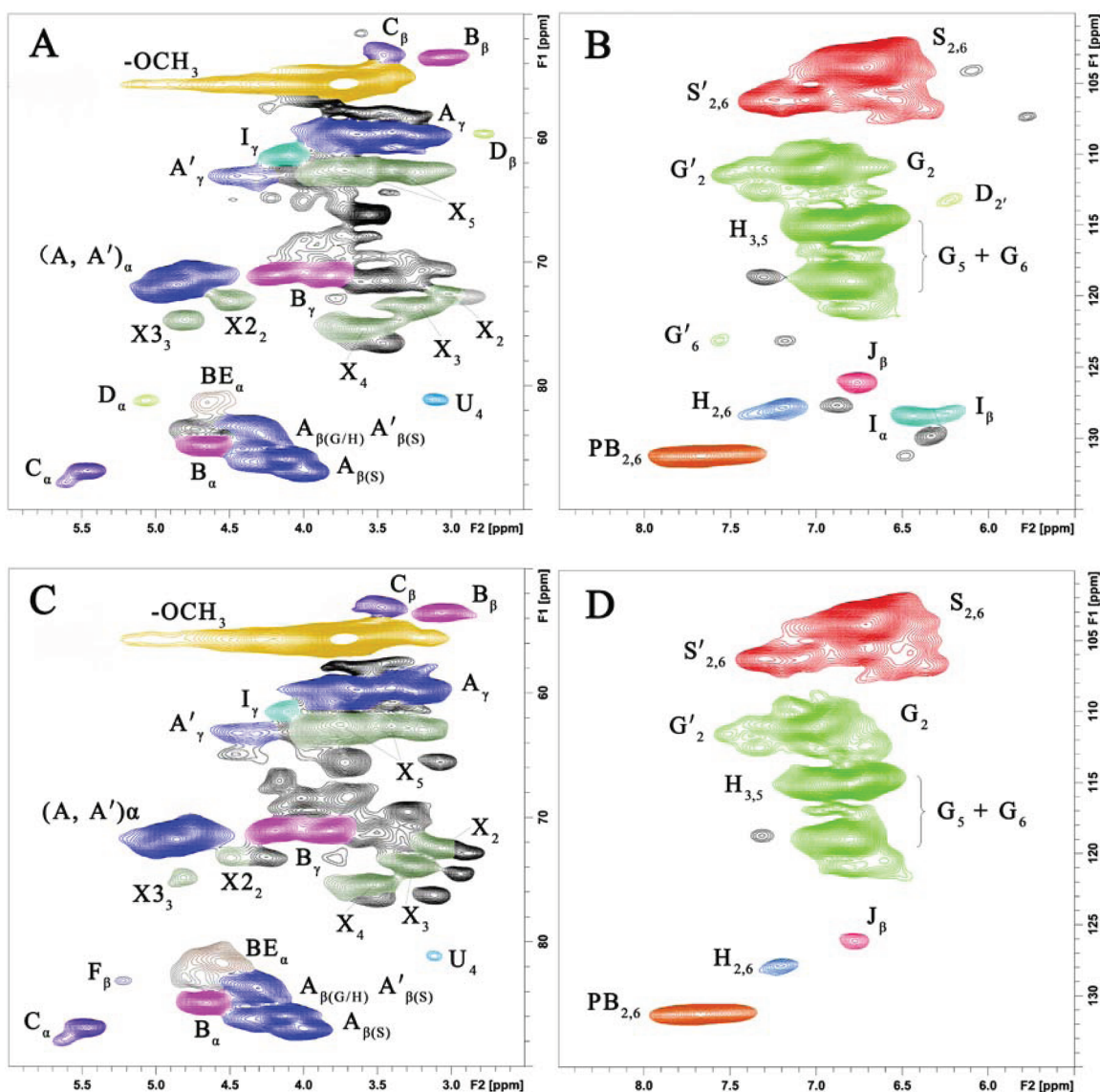


**Figure 2.** Side-chain (left column) and aromatic regions (right column) in the 2D HSQC NMR spectra:  $\delta_C/\delta_H$  50–90/2.5–6.0 and  $\delta_C/\delta_H$  100–135/5.5–8.5, respectively. (A, B) Milled wood lignin (MWL); (C, D) mild acidolysis lignin (MAL). Symbols are taken from Figure 3. See Table 3 for signal assignment.

in structures A linked to G/H lignin units and  $\gamma$ -acylated  $\beta$ -O-4' aryl ether substructures (A') linked to S lignin units. The  $C_\gamma$ - $H_\gamma$  correlations in structures A were observed at  $\delta_C/\delta_H$  59.5–59.7/3.40–3.63. The  $C_\gamma$ - $H_\gamma$  correlations in  $\gamma$ -acylated lignin units (A') were observed at  $\delta_C/\delta_H$  63.2/4.33–4.49. These signals indicated that lignin in triploid of *Populus tomentosa* Carr. is partially acylated at the  $\gamma$ -carbon in  $\beta$ -O-4' aryl ether linkages of the side chains.<sup>39,40</sup> Besides, a small signal at  $\delta_C/\delta_H$  83.1/5.21 was observed in the side-chain region of MAL, which corresponded to the  $C_\beta$ - $H_\beta$  correlations in oxidized ( $C_\alpha=O$ )  $\beta$ -O-4' substructures F. However, these correlations could only be seen at lower contour levels in the side-chain region of MWL (not shown).

In addition, strong signals for resinol ( $\beta$ - $\beta'$ ) substructures B were observed with their  $C_\alpha$ - $H_\alpha$ ,  $C_\beta$ - $H_\beta$ , and the double  $C_\gamma$ - $H_\gamma$  correlations at  $\delta_C/\delta_H$  84.8/4.65, 53.5/3.06, and 71.0/4.18 and/3.82, respectively. The  $C_\alpha$ - $H_\alpha$  and  $C_\beta$ - $H_\beta$  correlations in phenylcoumaran ( $\beta$ -5') substructures C were discovered

at  $\delta_C/\delta_H$  86.8/5.46 and 53.3/3.46, respectively, whereas the  $C_\gamma$ - $H_\gamma$  correlations were overlapped with other signals around  $\delta_C/\delta_H$  62.5/3.73. Moreover, small signals corresponding to spirodienone ( $\beta$ -1') substructures D could be observed in the side-chain region of MWL and disappeared in the side-chain region of MAL. Their  $C_\alpha$ - $H_\alpha$  and  $C_\beta$ - $H_\beta$  correlations were detected at  $\delta_C/\delta_H$  81.2/5.07 and 59.7/2.77, respectively. The  $C_\beta$ - $H_\beta$  correlations in spirodienone substructures D ( $\delta_C/\delta_H$  79.5/4.12) could only be discovered at lower contour levels (not shown). Finally, the  $C_\gamma$ - $H_\gamma$  correlations in *p*-hydroxycinnamyl alcohol end groups (substructures I) were observed at  $\delta_C/\delta_H$  61.4/4.10 in the side-chain region of both MWL and MAL.

**Aromatic Regions.** The main cross-signals in the aromatic region of the 2D HSQC spectra of MWL and MAL corresponded to the aromatic rings of *p*-hydroxyphenyl (H), syringyl (S), and guaiacyl (G) lignin units, as well as some lignin substructures. The S-lignin units showed a prominent signal for the  $C_{2,6}$ - $H_{2,6}$  correlations at  $\delta_C/\delta_H$  103.8/6.71, whereas

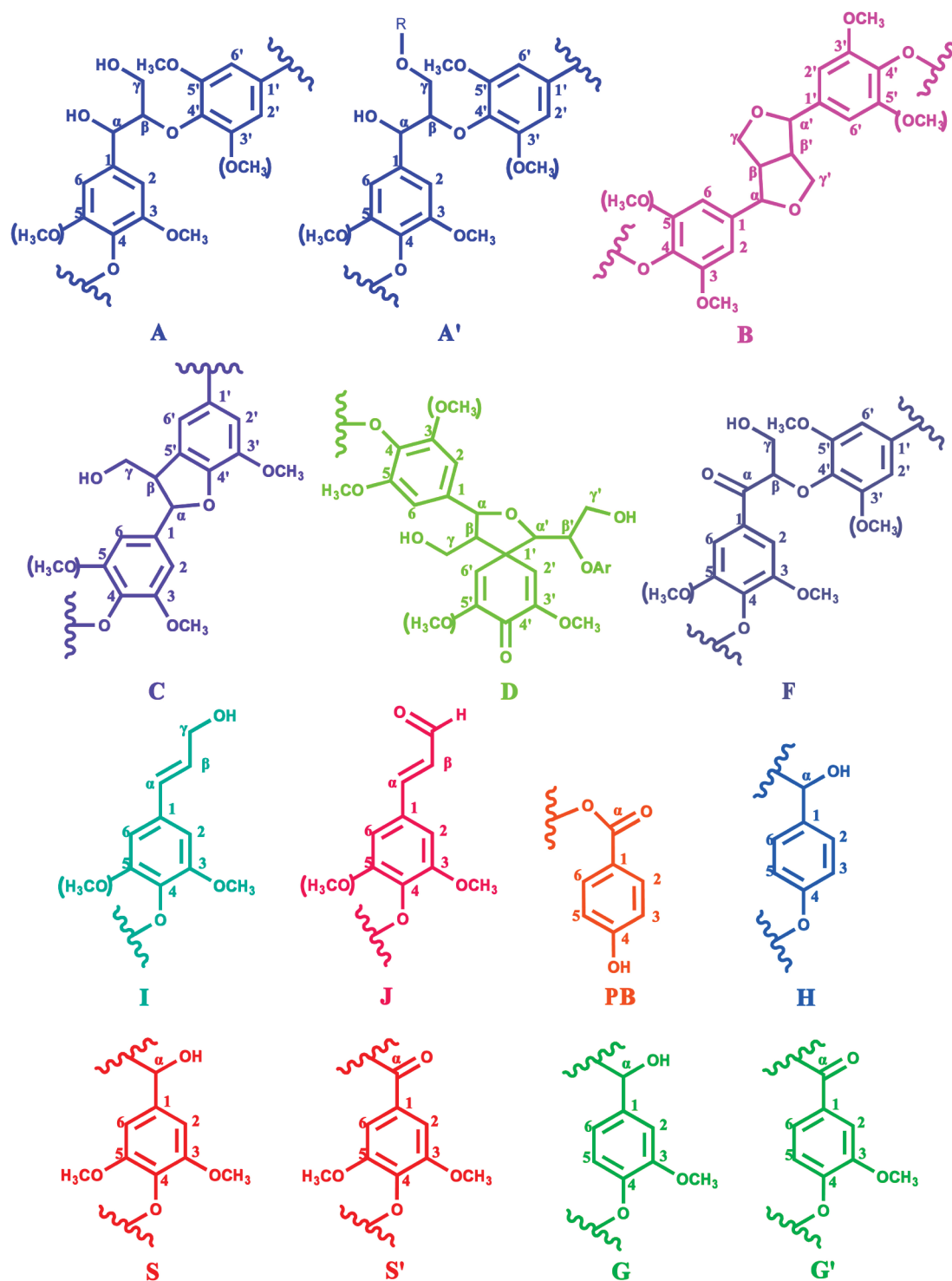


**Figure 3.** Main classical and acylated lignin substructures, involving different side-chain linkages, and aromatic units identified by 2D NMR of milled wood lignin (MWL) and mild acidolysis lignin (MAL): (A)  $\beta$ -O-4' aryl ether linkages with a free  $-\text{OH}$  at the  $\gamma$ -carbon; (A')  $\beta$ -O-4' aryl ether linkages with acetylated and/or *p*-hydroxybenzoated  $-\text{OH}$  at  $\gamma$ -carbon; (B) resinol substructures formed by  $\beta$ - $\beta'$ ,  $\alpha$ -O- $\gamma'$ , and  $\gamma$ -O- $\alpha'$  linkages; (C) phenylcoumarane substructures formed by  $\beta$ - $S'$  and  $\alpha$ -O-4' linkages; (D) spirodienone substructures formed by  $\beta$ -1' and  $\alpha$ -O- $\alpha'$  linkages; (F)  $C_\alpha$ -oxidized  $\beta$ -O-4' substructures; (I) *p*-hydroxycinnamyl alcohol end groups; (J) cinnamaldehyde end groups; (PB) *p*-hydroxybenzoate substructures; (H) *p*-hydroxyphenyl units; (G) guaiacyl units; (S) syringyl units; (S') oxidized syringyl units with a  $C_\alpha$  ketone; (G') oxidized guaiacyl units with a  $\alpha$ -ketone.

the  $C_{2,6}-H_{2,6}$  correlations in  $C_\alpha$ -oxidized S units (S') were observed at  $\delta_C/\delta_H$  106.2/7.23. The G units showed different correlations for  $C_2-H_2$ ,  $C_5-H_5$ , and  $C_6-H_6$  at  $\delta_C/\delta_H$  110.9/6.98, 114.9/6.77, and 119.0/6.80, respectively. The correlations

for the  $C_2-H_2$  and  $C_6-H_6$  in oxidized  $\alpha$ -ketone structures G' were observed at  $\delta_C/\delta_H$  111.4/7.51 and 118.9/6.07, respectively. A minor  $C_{2,6}-H_{2,6}$  aromatic correlation from H units was clearly observed at  $\delta_C/\delta_H$  127.9/7.19, but the  $C_{3,5}-H_{3,5}$

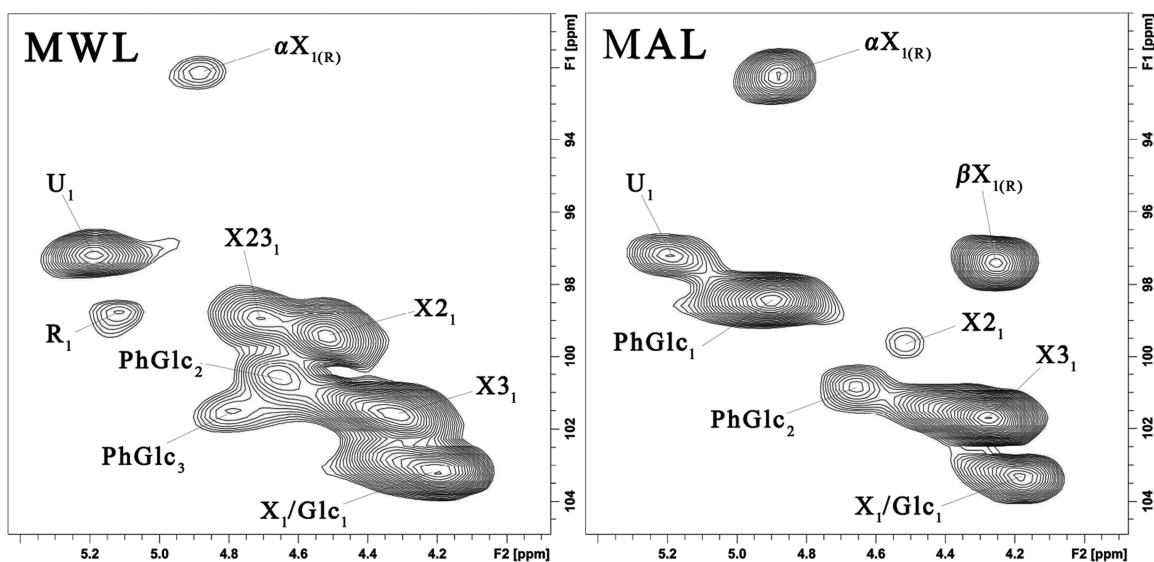


**Figure 4.** Carbohydrate anomeric regions ( $\delta_C/\delta_H$  90–105/3.9–5.4) of 2D HSQC NMR spectra of the lignin fractions. Assignments of the carbohydrate signals are listed in Table 4.

**Table 3.** Assignment of Main Lignin  $^{13}\text{C}$ – $^1\text{H}$  Cross-Signals in the HSQC Spectra of the Lignin Fractions

label	$\delta_C/\delta_H$	assignment
$C_\beta$	53.3/3.46	$C_\beta$ – $H_\beta$ in phenylcoumarane substructures (C)
$B_\beta$	53.5/3.06	$C_\beta$ – $H_\beta$ in resinol substructures (B)
–OCH <sub>3</sub>	55.6/3.73	C–H in methoxyls
$D_\beta$	59.7/2.77	$C_\beta$ – $H_\beta$ in spirodienone substructures (D)
$A_\gamma$	59.5–59.7/3.40–3.63	$C_\gamma$ – $H_\gamma$ in $\beta$ -O-4' substructures (A)
$I_\gamma$	61.4/4.10	$C_\gamma$ – $H_\gamma$ in <i>p</i> -hydroxycinnamyl alcohol end groups (I)
$C_\gamma$	62.5/3.73	$C_\gamma$ – $H_\gamma$ in phenylcoumaran substructures (C)
$A'_\gamma$	63.2/4.33–4.49	$C_\gamma$ – $H_\gamma$ in $\gamma$ -acylated $\beta$ -O-4' substructures ( $A'$ and $A''$ )
$B_\gamma$	71.0/3.82 and 4.18	$C_\gamma$ – $H_\gamma$ in resinol substructures (B)
(A, A') $_\alpha$	71.8/4.86	$C_\alpha$ – $H_\alpha$ in $\beta$ -O-4' substructures (A) and $\gamma$ -acylated $\beta$ -O-4' substructures ( $A'$ )
$D_{\beta'}$	79.5/4.12	$C_{\beta'}$ – $H_{\beta'}$ in spirodienone substructures (D)
$D_\alpha$	81.2/5.07	$C_\alpha$ – $H_\alpha$ in spirodienone substructures (D)
$F_\beta$	83.1/5.21	$C_\beta$ – $H_\beta$ in oxidized ( $C_\alpha=O$ ) $\beta$ -O-4' substructures (F)
$A_{\beta(G/H)}$	83.9/4.29	$C_\beta$ – $H_\beta$ in $\beta$ -O-4' substructures linked to G and H units (A)
(A') $_{\beta(S)}$	83.9/4.29	$C_\beta$ – $H_\beta$ in $\gamma$ -acylated $\beta$ -O-4' substructures linked to S units ( $A'$ )
$B_\alpha$	84.8/4.65	$C_\alpha$ – $H_\alpha$ in resinol substructures (B)
$A_{\beta(S)}$	85.9/4.12	$C_\beta$ – $H_\beta$ in $\beta$ -O-4' substructures linked to S units (A)
$C_\alpha$	86.8/5.46	$C_\alpha$ – $H_\alpha$ in phenylcoumaran substructures (C)
$S_{2,6}$	103.8/6.71	$C_{2,6}$ – $H_{2,6}$ in etherified syringyl units (S)
$S'_{2,6}$	106.2/7.23 and 7.07	$C_{2,6}$ – $H_{2,6}$ in oxidized ( $C_\alpha=O$ ) syringyl units ( $S'$ )
$G_2$	110.9/6.98	$C_2$ – $H_2$ in guaiacyl units (G)
$G'_2$	111.4/7.51	$C_2$ – $H_2$ in oxidized ( $C_\alpha=O$ ) guaiacyl units ( $G'$ )
$D'_2$	113.3/6.22	$C_{2'}$ – $H_{2'}$ in spirodienone substructures (D)
$G_5$	114.9/6.77	$C_2$ – $H_2$ in guaiacyl units (G)
$D'_6$	118.9/6.07	$C_{6'}$ – $H_{6'}$ in spirodienone substructures (D)
$G_6$	119.0/6.80	$C_6$ – $H_6$ in guaiacyl units (G)
$G'_6$	123.3/7.60	$C_6$ – $H_6$ in oxidized ( $C_\alpha=O$ ) guaiacyl units ( $G'$ )
$J_\beta$	126.1/6.76	$C_\beta$ – $H_\beta$ in cinnamaldehyde end groups (J)
$H_{2,6}$	127.9/7.19	$C_{2,6}$ – $H_{2,6}$ in <i>p</i> -hydroxyphenyl units (H)
$I_\beta$	128.2/6.25	$C_\beta$ – $H_\beta$ in <i>p</i> -hydroxycinnamyl alcohol end groups (I)
$I_\alpha$	128.4/6.44	$C_\alpha$ – $H_\alpha$ in <i>p</i> -hydroxycinnamyl alcohol end groups (I)
$PB_{2,6}$	131.2/7.67	$C_{2,6}$ – $H_{2,6}$ in <i>p</i> -hydroxybenzoate substructures (PB)
$J_\alpha$	153.5/7.60	$C_\alpha$ – $H_\alpha$ in cinnamaldehyde end groups (J)

position correlations were overlapped with those from guaiacyl 5-positions.

Other signals in the aromatic regions were also observed and assigned to *p*-hydroxybenzoate substructures (PB), *p*-hydroxycinnamyl alcohol end groups (I), cinnamaldehyde end groups (J), and spirodienone substructures (D). The C<sub>2,6</sub>–H<sub>2,6</sub> correlations of PB were observed as a strong signal at  $\delta_C/\delta_H$  131.2/7.67. It has been reported that PB is considered to exclusively acylate the  $\gamma$ -position of S-lignin side chains, analogously with *p*-coumarates (pCA) in grasses.<sup>55,56</sup> The signals for the C <sub>$\alpha$</sub> –H <sub>$\alpha$</sub>  and C <sub>$\beta$</sub> –H <sub>$\beta$</sub>  correlations of substructures I were clearly discovered at  $\delta_C/\delta_H$  128.4/6.44 and 128.2/6.25, respectively, in the aromatic region of the HSQC spectrum of MWL. However, these signals could only be seen at lower contour levels in the spectrum of MAL (not shown). The signals for the C <sub>$\alpha$</sub> –H <sub>$\alpha$</sub>  and

C <sub>$\beta$</sub> –H <sub>$\beta$</sub>  correlations of substructures J were found at  $\delta_C/\delta_H$  153.5/7.60 (not shown) and 126.1/6.76, respectively. In the aromatic region of the HSQC spectrum of MWL, the weak signal for the C<sub>2'</sub>–H<sub>2'</sub> correlations of spirodienone substructures D was clearly discovered at  $\delta_C/\delta_H$  113.3/6.22, whereas its C<sub>6'</sub>–H<sub>6'</sub> correlations ( $\delta_C/\delta_H$  118.9/6.07) could be seen only at lower contour levels (not shown). In accordance with the discussion in the side-chain region of the HSQC spectrum of MAL, no C<sub>2'</sub>–H<sub>2'</sub> or C<sub>6'</sub>–H<sub>6'</sub> correlations of substructures D could be detected.

**Associated Carbohydrates.** Various signals from the associated carbohydrates could also be found in the HSQC spectra of MWL and MAL, including signals in the aliphatic regions and anomeric regions. In the aliphatic regions (Figure 2, left column), the C<sub>2</sub>–H<sub>2</sub> correlations from 2-*O*-acetyl- $\beta$ -D-xylopyranoside units (X<sub>2</sub>) and C<sub>3</sub>–H<sub>3</sub> correlations from 3-*O*-acetyl- $\beta$ -D-xylopyranoside units (X<sub>3</sub>) were clearly observed at  $\delta_C/\delta_H$  73.2/4.49 and 74.7/4.80, respectively. Other signals from  $\beta$ -D-xylopyranoside units (X) were evidently noted, with its C<sub>2</sub>–H<sub>2</sub>, C<sub>3</sub>–H<sub>3</sub>, and C<sub>4</sub>–H<sub>4</sub> correlations at  $\delta_C/\delta_H$  72.5/3.02, 73.7/3.22, and 75.4/3.60, respectively, but the C<sub>5</sub>–H<sub>5</sub> correlations from X were observed at  $\delta_C/\delta_H$  62.6/3.40 and 3.72, which were overlapped with other unassigned cross-signals. The C<sub>4</sub>–H<sub>4</sub> correlations from 4-*O*-methyl- $\alpha$ -D-GlcUA (U<sub>4</sub>) were observed at  $\delta_C/\delta_H$  81.1/3.10. All of these were well in line with the results of carbohydrate analysis as shown in Table 1. These results confirmed that acetylated 4-*O*-methylglucoxytan is the major carbohydrate associated with lignin macromolecules, and acetyl groups frequently acylate the C2 and C3 positions.<sup>53</sup>

Benzyl ether (BE) LCC linkages could also be detected in the aliphatic regions, and the main lignin–carbohydrate linkages are given in Figure 5.<sup>10,11</sup> Previous studies based on lignin–carbohydrate model compounds have found that the BE LCC structures can be divided into two types: (a) BE<sub>1</sub>, linkages between the  $\alpha$ -position of lignin and primary OH groups of carbohydrates (at C-6 of Glc, Gal, and Man, and C-5 of Ara); and (b) BE<sub>2</sub>, linkages between the  $\alpha$ -position of lignin and secondary OH groups of carbohydrates, mainly of lignin–xylan type.<sup>57–59</sup> In the present study, the C <sub>$\alpha$</sub> –H <sub>$\alpha$</sub>  correlations in BE LCC structures were found at  $\delta_C/\delta_H$  81.3/4.65 in the HSQC spectra of both MWL and MAL. Besides, signals for benzyl ester bonds at  $\sim 75$ – $77/6.0$ – $6.2$  ppm were not detected.<sup>10,11,60</sup>

**Table 4. Assignment of the Associated Carbohydrate <sup>13</sup>C–<sup>1</sup>H Cross-Signals in the HSQC Spectra of the Lignin Fractions**

label	$\delta_C/\delta_H$	assignment
X <sub>5</sub>	62.6/3.40 and 3.72	C <sub>5</sub> –H <sub>5</sub> in $\beta$ -D-xylopyranoside
X <sub>2</sub>	72.5/3.02	C <sub>2</sub> –H <sub>2</sub> in $\beta$ -D-xylopyranoside
X <sub>2</sub> <sub>2</sub>	73.2/4.49	C <sub>2</sub> –H <sub>2</sub> in 2- <i>O</i> -acetyl- $\beta$ -D-xylopyranoside
X <sub>3</sub>	73.7/3.22	C <sub>3</sub> –H <sub>3</sub> in $\beta$ -D-xylopyranoside
X <sub>3</sub> <sub>3</sub>	74.7/4.80	C <sub>3</sub> –H <sub>3</sub> in 3- <i>O</i> -acetyl- $\beta$ -D-xylopyranoside
X <sub>4</sub>	75.4/3.60	C <sub>4</sub> –H <sub>4</sub> in $\beta$ -D-xylopyranoside
U <sub>4</sub>	81.1/3.10	C <sub>4</sub> –H <sub>4</sub> in 4- <i>O</i> -methyl- $\alpha$ -D-GlcUA
BE <sub><math>\alpha</math></sub>	81.3/4.65	C <sub><math>\alpha</math></sub> –H <sub><math>\alpha</math></sub> in benzyl ether LCC structures
anomeric correlations (C <sub>1</sub> –H <sub>1</sub> )		
$\alpha$ X <sub>1(R)</sub>	92.2/4.88	(1 $\rightarrow$ 4)- $\alpha$ -D-xylopyranoside (R)
U <sub>1</sub>	97.2/5.18	4- <i>O</i> -methyl- $\alpha$ -D-GlcUA
$\beta$ X <sub>1(R)</sub>	97.4/4.26	(1 $\rightarrow$ 4)- $\beta$ -D-xylopyranoside (R)
PhGlc <sub>1</sub>	98.4/4.90	phenyl glycoside linkages
R <sub>1</sub>	98.8/5.12	(1 $\rightarrow$ 2)- $\alpha$ -L-rhamnopyranoside
X <sub>2</sub> <sub>3</sub>	98.9/4.71	2,3- <i>O</i> -acetyl- $\beta$ -D-xylopyranoside
X <sub>2</sub> <sub>1</sub>	99.4/4.52	2- <i>O</i> -acetyl- $\beta$ -D-xylopyranoside
PhGlc <sub>2</sub>	100.6/4.65	phenyl glycoside linkages
PhGlc <sub>3</sub>	101.5/4.79	phenyl glycoside linkages
X <sub>3</sub> <sub>1</sub>	101.6/4.32	3- <i>O</i> -acetyl- $\beta$ -D-xylopyranoside
X <sub>1</sub> /Glc <sub>1</sub>	103.2/4.20	$\beta$ -D-xylopyranoside/ $\beta$ -D-glucopyranoside

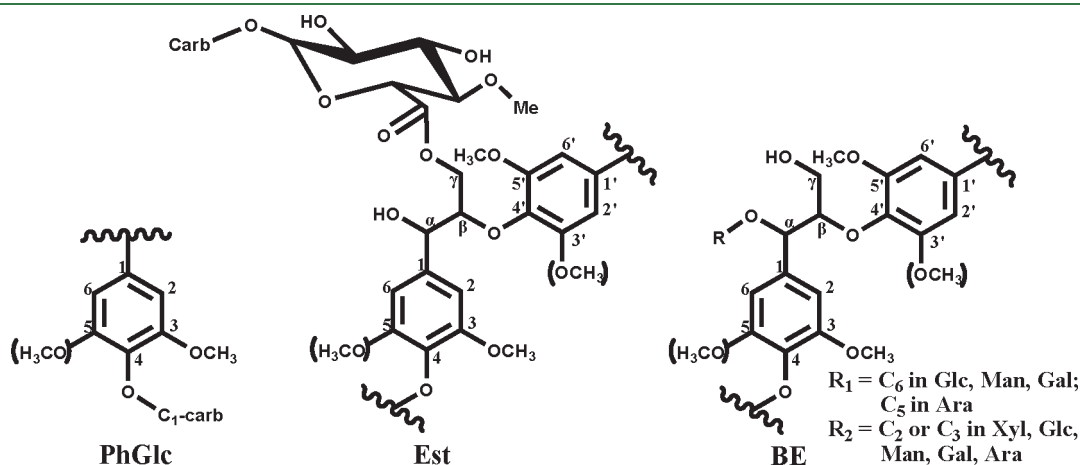


**Figure 5.** Main lignin–carbohydrate linkages: PhGlc, phenyl glycoside; Est,  $\gamma$ -ester; and BE, benzyl ether.

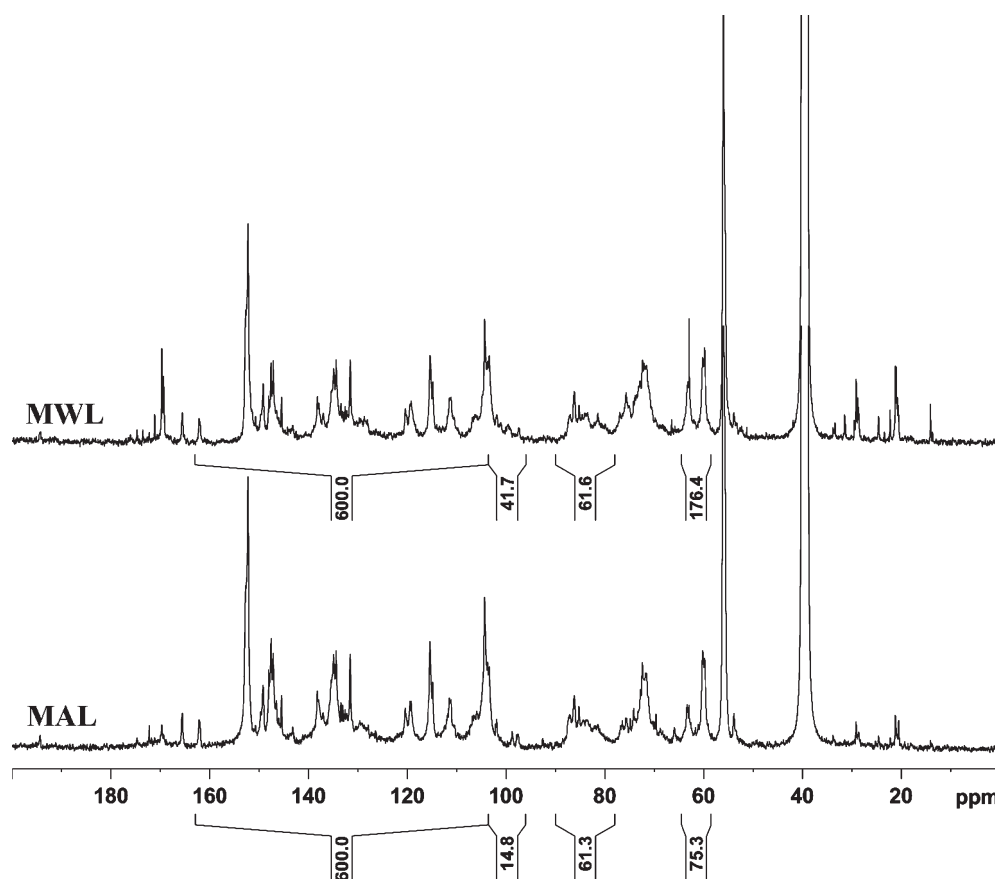


**Figure 6.** Quantitative  $^{13}\text{C}$  NMR spectra of milled wood lignin (MWL) and mild acidolysis lignin (MAL).

The well-resolved anomeric correlations ( $\delta_{\text{C}}/\delta_{\text{H}}$  90–105/3.9–5.4) of the associated carbohydrates are shown in Figure 4. The assignments of the anomeric correlations were based on the published literature (Table 4).<sup>10,11,53</sup> As discussed above, the corresponding anomeric correlations ( $\text{C}_1\text{--H}_1$ ) of  $\beta$ -D-xylopyranoside units acetylated at C-2 (X2), C-3 (X3), or both positions (X23) were observed at  $\delta_{\text{C}}/\delta_{\text{H}}$  99.4/4.52, 101.6/4.32, 98.9/4.71, respectively. The corresponding anomeric correlations of  $\beta$ -D-xylopyranoside units (X<sub>1</sub>) were found at  $\delta_{\text{C}}/\delta_{\text{H}}$  103.2/4.20, whereas the minor anomeric correlations of  $\beta$ -D-glucopyranoside units (Glc<sub>1</sub>) might be overlapped in this region. The anomeric correlations from the reducing end of (1→4)- $\alpha$ -D-xylopyranoside ( $\alpha\text{X}_1$ ) and (1→4)- $\beta$ -D-xylopyranoside ( $\beta\text{X}_1$ ) units were found at  $\delta_{\text{C}}/\delta_{\text{H}}$  92.2/4.88 and 97.4/4.26, respectively. Besides, the anomeric correlations from 4-O-methyl- $\alpha$ -D-GlcUA (U<sub>1</sub>) and (1→2)- $\alpha$ -L-rhamnopyranoside units (R<sub>1</sub>) were clearly observed at  $\delta_{\text{C}}/\delta_{\text{H}}$  97.2/5.18 and 98.8/5.12, respectively. According to a previous study,<sup>11</sup> other unassigned correlations in the anomeric regions belong to phenyl glycoside linkage units. Detailed assignments of these dispersed contours need to be made in future studies using models and a variety of well-characterized polysaccharide polymers.<sup>53</sup> In the present study, these cross-signals were labeled PhGlc<sub>1</sub>, PhGlc<sub>2</sub>, and PhGlc<sub>3</sub>, and their correlations were observed at  $\delta_{\text{C}}/\delta_{\text{H}}$  98.4/4.90, 100.6/4.65, and 101.5/4.79, respectively.

**Quantification of Lignin Structures and LCC Linkages.** Quantification of lignin structures and LCC linkages is very important. These efforts provide not only more comprehensive information about lignin architecture and reactivity but also an

appropriate method for the selective separation and isolation of lignin and carbohydrate preparations from lignocellulosics.<sup>11,15</sup> However, the quantitative  $^{13}\text{C}$  NMR, which has been successfully developed to quantify the lignin structures, is unsuitable when the lignin preparation contains high LCC fractions. In the present study, the quantification method by the combination of quantitative  $^{13}\text{C}$  and 2D HSQC NMR, which was proposed by Zhang and Gellerstedt,<sup>17</sup> was adopted to quantify the lignin structures. Figure 6 shows the quantitative  $^{13}\text{C}$  NMR spectra of MWL and MAL. A detailed assignment of the various signals in the quantitative  $^{13}\text{C}$  NMR spectra was given in our earlier studies.<sup>39,40</sup>

The key point in the quantification method adopted was to select a suitable internal standard reference signal originating from lignin with similar structural features.<sup>17</sup> The selected internal standard references can convert relative integration values obtained from the corresponding 2D spectrum to the absolute values. As the integral values in Figure 6, the resonance for the total aromatic carbons (163.0–103.6 ppm) was assigned as 600.0. The integral values for the selected internal standard references and other structural moieties were expressed per 100 Ar. To quantify the lignin structures and LCC linkages, the values obtained from the integration of three clusters at 103.6–96.0, 90.0–78.0, and 64.5–58.5 ppm in the corresponding quantitative  $^{13}\text{C}$  spectra were used, and the results are also listed in Figure 6. The amounts of lignin substructures and LCC moieties were calculated per 100 Ar as follows:<sup>11,17</sup>

$$\text{PhGlc} = 2D_{(\text{R}_1+\text{PhGlc})} / 2D_{(103.6-96.0/5.40-3.90)} \\ \times {}^{13}\text{C}_{(103.6-96.0)} / {}^{13}\text{C}_{(163.0-103.6)} \times 600$$



**Table 5. Lignin and LCC Linkage Characteristics from Integration of Quantitative  $^{13}\text{C}$  and 2D HSQC NMR Spectra of the Lignin Fractions: Results Expressed per 100 Ar (and as Percentage of Total Side Chains)**

characteristic	MWL	MAL
linkages (% side chains involved)		
$\beta$ -O-4' aryl ether (A)	41.5 (60.9)	43.3 (70.4)
resinol (B)	14.6 (21.4)	12.7 (20.7)
phenylcoumaran (C)	3.7 (5.4)	4.0 (6.5)
spirodienones (D)	0.7 (1.0)	0 (0)
$\beta$ -O-4' oxidized at $\text{C}_\alpha$ (F)	0.2 (0.3)	0.6 (1.0)
<i>p</i> -hydroxycinnamyl alcohol end groups (I)	7.4 (10.9)	0.9 (1.5)
percentage of $\gamma$ -acylation ( $\beta$ -O-4')	7.5	2.9
S/G ratio	1.57	1.62
LCC linkages		
PhGlc	4.1	4.5
BE	2.1	5.8
Est <sup>a</sup>	3.4	1.3

<sup>a</sup> Sum of LCC  $\gamma$ -ester (Est) and  $\gamma$ -acylated  $\beta$ -O-4' aryl ether substructures (A').

$$\text{BE} = 2D_{(\text{BE}\alpha)} / 2D_{(90.0-78.0/6.00-2.50)} \times {}^{13}\text{C}_{(90.0-78.0)} / {}^{13}\text{C}_{(163.0-103.6)} \times 600$$

$$\text{Est} = 2D_{(\text{A}'\gamma)} / 2D_{(64.5-58.5/5.0-2.5)} \times {}^{13}\text{C}_{(64.5-58.5)} / {}^{13}\text{C}_{(163.0-103.6)} \times 600$$

PhGlc, BE, and Est are the amounts of phenyl glycoside, benzyl ether, and  $\gamma$ -ester LCC linkages (per 100 Ar). The amounts of the various lignin substructures were calculated according to the formula of BE. For resinol (B), phenylcoumarane (C), and spirodienone (D) substructures, the  $\text{C}_\alpha$ - $\text{H}_\alpha$  correlations in the 2D spectrum were used, whereas the  $\text{C}_\beta$ - $\text{H}_\beta$  correlations were selected for substructures A, A', and F. It should be noted that the amount of  $\gamma$ -ester LCC linkages calculated was the sum of LCC  $\gamma$ -ester (Est) and  $\gamma$ -acylated  $\beta$ -O-4' aryl ether substructures (A'). Signals for ester bonds at the  $\gamma$ -position of the  $\text{C}_9$  unit, probably between the  $\gamma$ -position of lignin and a carboxyl group of uronic acid,<sup>60</sup> were overlapped with the signals from  $\gamma$ -acylated  $\beta$ -O-4' aryl ether substructures (A'). The overlapped signals between these two substructures have been distinguished by using high-resolution NMR spectroscopy (950 MHz) with CryoProbe.<sup>11</sup> The results on the quantification of lignin substructures and LCC linkages in MWL and MAL are summarized in Table 5.

As can be seen from Table 5, MWL and MAL exhibited similar structural features. The main substructures present in both MWL and MAL were  $\beta$ -O-4' aryl ether (A), resinol (B), and phenylcoumaran (C) substructures, and their abundances per 100 Ar units changed from 41.5 to 43.3, from 14.6 to 12.7, and from 3.7 to 4.0, respectively. The S/G ratios were very close, estimated to be 1.57 and 1.62 for MWL and MAL, respectively. However, some different structural features between MWL and MAL were also quantified. MWL contained a low amount of spirodienone (D) substructures, 0.7 per 100 Ar, whereas this substructure could not be detected in the preparation of MAL. It is worth

noting that the amounts of  $\text{C}_\alpha$ -oxidized  $\beta$ -O-4' substructures (F) and *p*-hydroxycinnamyl alcohol end groups (I) were different in these two lignin preparations. Whereas the former increased from 0.2 to 0.6 per 100 Ar, the latter decreased from 7.4 to 0.9 per 100 Ar. These differences might be due to the different isolation methods used for preparing the lignin fractions. For MWL, the occurrence of  $\text{C}_\alpha$ -oxidized  $\beta$ -O-4' substructures (F) might be due to the ball-milling process. It has been reported that the effect of ball-milling could result in oxidation reactions of the lignin side chains.<sup>7,41,61</sup> However, the increase of F substructures and the decrease of I in MAL could be attributed to the mild acid hydrolysis.

The main types of LCC linkages in wood are believed to be phenyl glycoside bonds, esters, and benzyl ethers.<sup>8-11</sup> Both benzyl ethers and phenyl glycoside linkages can be easily cleaved under mild acidic conditions.<sup>27</sup> However, in the present study, all of these linkages have been detected both in MWL and in MAL (Table 5). Specifically, the amounts of PhGlc and BE in MWL were slightly higher than in MAL. As aforementioned, this could be explained by the different isolation methods used.<sup>24,31,42,43</sup> Besides, the BE in MAL might be rich in nonphenolic, because the nonphenolic BE was found to be more stable under such conditions.<sup>62,63</sup>

In summary, MAL has been sequentially isolated from the residual wood meal after extraction of MWL from the ball-milled poplar wood. The results indicated that MWL and MAL exhibited similar structural features. Therefore, they could be combined to understand the structure of a greater proportion of lignin in the cell wall. The method to quantify the different lignin structures and LCC linkages by using a combination of quantitative  $^{13}\text{C}$  and 2D HSQC NMR techniques was proved to be effective when the lignin preparation with high amounts of associated carbohydrates. However, for accurate assignment of the associated carbohydrates and LCC linkages, future studies using model compounds and a variety of well-characterized polysaccharide polymer are needed.

## AUTHOR INFORMATION

### Corresponding Author

\*Phone: +86-10-62336903. Fax: +86-10-62336903. E-mail: (F.X.) xfx315@bjfu.edu.cn or (R.-C.S.) rcsun3@bjfu.edu.cn.

### Funding Sources

We are grateful for the financial support of this research from the Specific Programs in Graduate Science and Technology Innovation of Beijing Forestry University (No. BLYJ201113), State Forestry Administration (200804015, 20100400706), Major State Basic Research Projects of China (973-2010CB732204), National Science Foundation of China (30930073, 31110103902), and China Ministry of Education (111).

## REFERENCES

- (1) Higuchi, T. *Biochemistry and Molecular Biology of Wood*; Springer-Verlag: London, U.K., 1997.
- (2) Boerjan, W.; Ralph, J.; Baucher, M. Lignin biosynthesis. *Annu. Rev. Plant Biol.* **2003**, *54*, 519-546.
- (3) Ralph, J.; Lundquist, K.; Brunow, G.; Lu, F. C.; Kim, H.; Schatz, P. F.; Marita, J. M.; Hatfield, R. D.; Ralph, S. A.; Christensen, J. H.; Boerjan, W. Lignins: natural polymers from oxidative coupling of 4-hydroxyphenylpropanoids. *Phytochem. Rev.* **2004**, *3*, 29-60.
- (4) Zhao, Q.; Dixon, R. A. Transcriptional networks for lignin biosynthesis: more complex than we thought? *Trends Plant Sci.* **2011**, *16*, 227-233.

- (5) Li, X.; Weng, J. K.; Chapple, C. Improvement of biomass through lignin modification. *Plant J.* **2008**, *54*, 569–581.
- (6) Studer, M. H.; DeMartini, J. D.; Davis, M. F.; Sykes, R. W.; Davison, B.; Keller, M.; Tuskan, G. A.; Wyman, C. E. Lignin content in natural *Populus* variants affects sugar release. *Proc. Natl. Acad. Sci. U.S.A.* **2011**, *108*, 6300–6305.
- (7) Ikeda, T.; Holtman, K.; Kadla, J. F.; Chang, H.-m.; Jameel, H. Studies on the effect of ball milling on lignin structure using a modified DFRC method. *J. Agric. Food Chem.* **2002**, *50*, 129–135.
- (8) Fengel, D.; Wegener, G. *Wood Chemistry, Ultrastructure and Reactions*; de Gruyter: Berlin, Germany, 1989.
- (9) Koshijima, T.; Watanabe, T. *Association between Lignin and Carbohydrates in Wood and Other Plant Tissues*; Springer: Berlin, Germany, 2003.
- (10) Balakshin, M. Y.; Capanema, E. A.; Chang, H.-m. MWL fraction with a high concentration of lignin–carbohydrate linkages: isolation and 2D NMR spectroscopic analysis. *Holzforchung* **2007**, *61*, 1–7.
- (11) Balakshin, M. Y.; Capanema, E. A.; Gracz, H.; Chang, H.-m.; Jameel, H. Quantification of lignin–carbohydrate linkages with high-resolution NMR spectroscopy. *Planta* **2011**, *233*, 1097–1110.
- (12) Landucci, L. L. Quantitative  $^{13}\text{C}$  NMR characterization of lignin. I. A methodology for high precision. *Holzforchung* **1985**, *39*, 355–359.
- (13) Xia, Z.; Akim, L. G.; Argyropoulos, D. S. Quantitative  $^{13}\text{C}$  NMR analysis of lignins with internal standards. *J. Agric. Food Chem.* **2001**, *49*, 3573–3578.
- (14) Holtman, K.; Chang, H.-m.; Kadla, J. Solution-state nuclear magnetic resonance study of the similarities between milled wood lignin and cellulolytic enzyme lignin. *J. Agric. Food Chem.* **2004**, *52*, 720–726.
- (15) Capanema, E. A.; Balakshin, M. Y.; Kadla, J. F. A comprehensive approach for quantitative lignin characterization by NMR spectroscopy. *J. Agric. Food Chem.* **2004**, *52*, 1850–1860.
- (16) Capanema, E. A.; Balakshin, M. Y.; Kadla, J. F. Quantitative characterization of a hardwood milled wood lignin by nuclear magnetic resonance spectroscopy. *J. Agric. Food Chem.* **2005**, *53*, 9639–9649.
- (17) Zhang, L. M.; Gellerstedt, G. Quantitative 2D HSQC NMR determination of polymer structures by selecting suitable internal standard references. *Magn. Reson. Chem.* **2007**, *45*, 37–45.
- (18) Björkman, A. Isolation of lignin from finely divided wood with neutral solvents. *Nature* **1954**, *174*, 1057–1058.
- (19) Hu, Z. J.; Yeh, T. F.; Chang, H.-m.; Matsumoto, Y.; Kadla, J. F. Elucidation of the structure of cellulolytic enzyme lignin. *Holzforchung* **2006**, *60*, 389–397.
- (20) Pew, J. C. Properties of powered wood and isolation of lignin by cellulolytic enzymes. *Tappi* **1957**, *40*, 553–558.
- (21) Chang, H.-m.; Cowling, E. B.; Brown, W.; Adler, E.; Miksche, G. Comparative studies on cellulolytic enzyme lignin and milled wood lignin of sweetgum and spruce. *Holzforchung* **1975**, *29*, 153–159.
- (22) Chen, Y.; Shimizu, Y.; Takai, M.; Hayashi, J. A method for isolation of milled-wood lignin involving solvent swelling prior to enzyme treatment. *Wood Sci. Technol.* **1995**, *29*, 295–306.
- (23) Zhang, A. P.; Lu, F. C.; Sun, R. C.; Ralph, J. Isolation of cellulolytic enzyme lignin from wood preswollen/dissolved in dimethyl sulfoxide/*N*-methylimidazole. *J. Agric. Food Chem.* **2010**, *58*, 3446–3450.
- (24) Wu, S.; Argyropoulos, D. S. An improved method for isolating lignin in high yield and purity. *J. Pulp Paper Sci.* **2003**, *29*, 235–240.
- (25) Guerra, A.; Filpponen, I.; Lucia, L. A.; Argyropoulos, D. S. Comparative evaluation of three lignin isolation protocols for various wood species. *J. Agric. Food Chem.* **2006**, *54*, 9696–9705.
- (26) Freudenberg, K. The constitution and biosynthesis of lignin. In *Molecular Biology Biochemistry and Biophysics*; Kleinszeller, A., Springer, G. F., Wittmann, H. G., Eds.; Springer-Verlag: Berlin, Germany, 1968; Vol. 2, pp 47–122.
- (27) Adler, E. Lignin chemistry: past, present and future. *Wood Sci. Technol.* **1977**, *11*, 169–218.
- (28) Sakakibara, A. Chemistry of lignin. In *Wood and Cellulose Chemistry*; Hon, D. N.-S., Shiraishi, N., Eds.; Dekker: New York, 1991; pp 113–175.
- (29) Lai, Y. Z.; Sarkanen, K. V. Isolation and structural studies. In *Lignins: Occurrence, Formation, Structure and Reactions*; Sarkanen, K. V., Ludvig, C. H., Eds.; Wiley-Interscience: New York, 1971; pp 165–240.
- (30) Eriksson, Ö.; Goring, D. A. I.; Lindgren, B. O. Structural studies on the chemical bonds between lignins and carbohydrates in spruce wood. *J. Wood Sci. Technol.* **1980**, *14*, 267–279.
- (31) Obst, J. Frequency and alkali resistance of lignin–carbohydrate bonds in wood. *Tappi* **1982**, *65*, 109–112.
- (32) Watanabe, T. Structural studies on the covalent bonds between lignin and carbohydrate in lignin–carbohydrate complexes by selective oxidation of the lignin with 2,3-dichloro-5,6-dicyano-1,4-benzoquinone. *Wood Res.* **1989**, *76*, 59–123.
- (33) Karlsson, O.; Ikeda, T.; Kishimoto, T.; Magara, K.; Matsumoto, Y.; Hosoya, S. Isolation of lignin–carbohydrate bonds in wood. Model experiments and preliminary application to pine wood. *J. Wood Sci.* **2004**, *50*, 142–150.
- (34) Heikkinen, S.; Toikka, M. M.; Karhunen, T.; Kilpeläinen, I. A. Quantitative 2D HSQC (Q-HSQC) via suppression of *J*-dependence of polarization transfer in NMR spectroscopy: application to wood lignin. *J. Am. Chem. Soc.* **2003**, *125*, 4362–4367.
- (35) Ibarra, D.; Chavez, M. I.; Rencoret, J.; Del Rio, J. C.; Gutierrez, A.; Romero, J.; Camarero, S.; Martinez, M. J.; Jumenez-Barbero, J.; Martinez, A. T. Lignin modification during *Eucalyptus globulus* kraft pulping followed by totally chlorine-free bleaching: a two dimensional nuclear magnetic resonance, Fourier transform infrared, and pyrolysis-gas chromatography/mass spectrometry study. *J. Agric. Food Chem.* **2007**, *55*, 3477–3490.
- (36) Ralph, J.; Akiyama, T.; Kim, H.; Lu, F. C.; Schatz, P. F.; Marita, J. M.; Ralph, S. A.; Reddy, M. S. S.; Chen, F.; Dixon, R. A. Effects of coumarate 3-hydroxylase down-regulation on lignin structure. *J. Biol. Chem.* **2006**, *281*, 8843–8853.
- (37) Sun, R. C.; Fang, J. M.; Tomkinson, J. Fractional isolation and structural characterization of lignins from oil palm trunk and empty fruit bunch fibres. *J. Wood Chem. Technol.* **1999**, *19*, 335–356.
- (38) Yuan, T. Q.; Xu, F.; He, J.; Sun, R. C. Structural and physico-chemical characterization of hemicelluloses from ultrasound-assisted extractions of partially delignified fast-growing poplar wood through organic solvent and alkaline solutions. *Biotechnol. Adv.* **2010**, *28*, 583–593.
- (39) Yuan, T. Q.; Sun, S. N.; Xu, F.; Sun, R. C. Isolation and physico-chemical characterization of lignins from ultrasound irradiated fast-growing poplar wood. *BioResources* **2011**, *6*, 414–433.
- (40) Yuan, T. Q.; Sun, S. N.; Xu, F.; Sun, R. C. Structural characterization of lignin from Triploid of *Populus tomentosa* Carr. *J. Agric. Food Chem.* **2011**, *59*, 6605–6615.
- (41) Guerra, A.; Filpponen, I.; Lucia, L.; Saquing, C.; Baumberger, S.; Argyropoulos, D. S. Toward a better understanding of the lignin isolation process from wood. *J. Agric. Food Chem.* **2006**, *54*, 5939–5947.
- (42) Enoki, A.; Yaku, F.; Koshijima, T. Synthesis of LCC model compounds and their chemical and enzymatic stabilities. *Holzforchung* **1983**, *37*, 135–141.
- (43) Juhást, T.; Szengyel, Z.; Réczey, K.; Siika-Aho, M.; Viikari, L. Characterization of cellulases and hemicellulases produced by *Trichoderma reesei* on various carbon sources. *Process Biochem.* **2005**, *40*, 3519–3525.
- (44) Furuno, H.; Takano, T.; Hirosawa, S.; Kamitakahara, H.; Nakatsubo, F. Chemical structure elucidation of total lignins in woods. Part II: Analysis of a fraction of residual wood left after MWL isolation and solubilized in lithium chloride/*N,N*-dimethylacetamide. *Holzforchung* **2006**, *60*, 653–658.
- (45) Jääskeläinen, A. S.; Sun, Y.; Argyropoulos, D. S.; Tamminen, T.; Hortling, B. The effect of isolation method on the chemical structure of residual lignin. *Wood Sci. Technol.* **2003**, *37*, 91–102.
- (46) Villaverde, J. J.; Li, J. B.; Ek, M.; Ligeró, P.; de Vega, A. Native lignin structure of *Miscanthus × giganteus* and its changes during acetic and formic acid fractionation. *J. Agric. Food Chem.* **2009**, *57*, 6262–6270.
- (47) del Río, J. C.; Rencoret, J.; Marques, G.; Gutiérrez, A.; Ibarra, D.; Santos, J. I.; Jiménez-Barbero, J.; Zhang, L. M.; Martínez, Á. T.

Highly acylated (acetylated and/or *p*-coumaroylated) native lignins from diverse herbaceous plants. *J. Agric. Food Chem.* **2008**, *56*, 9525–9534.

(48) del Río, J. C.; Rencoret, J.; Marques, G.; Li, J. B.; Gellerstedt, G.; Jiménez-Barbero, J.; Martínez, A. T.; Gutiérrez, A. Structural characterization of the lignin from jute (*Corchorus capsularis*) fibers. *J. Agric. Food Chem.* **2009**, *57*, 10271–10281.

(49) Lu, F. C.; Ralph, J. Non-degradative dissolution and acetylation of ball-milled plant cell walls: high-resolution solution-state NMR. *Plant J* **2003**, *35*, 535–544.

(50) Lu, F. C.; Ralph, J.; Morreel, K.; Messens, E.; Boerjan, W. Preparation and relevance of a cross-coupling product between sinapyl alcohol and sinapyl *p*-hydroxybenzoate. *Org. Biomol. Chem.* **2004**, *2*, 2888–2890.

(51) Martínez, A. T.; Rencoret, J.; Marques, G.; Gutiérrez, A.; Ibarra, D.; Jiménez-Barbero, J.; del Río, J. C. Monolignil acylation and lignin structure in some nonwoody plants: a 2D NMR study. *Phytochemistry* **2008**, *69*, 2831–2843.

(52) Rencoret, J.; Marques, G.; Gutiérrez, A.; Nieto, L.; Jiménez-Barbero, J.; Martínez, A. T.; del Río, J. C. Isolation and structural characterization of the milled-wood lignin from *Paulownia fortunei* wood. *Ind. Crops Prod.* **2009**, *30*, 137–143.

(53) Kim, H.; Ralph, J. Solution-state 2D NMR of ball-milled plant cell wall gels in DMSO-*d*<sub>6</sub>/pyridine-*d*<sub>5</sub>. *Org. Biomol. Chem.* **2010**, *8*, 576–591.

(54) Rencoret, J.; Gutiérrez, A.; Nieto, L.; Jiménez-Barbero, J.; Faulds, C. B.; Kim, H.; Ralph, J.; Martínez, A. T.; del Río, J. C. Lignin composition and structure in young versus adult *Eucalyptus globulus* plants. *Plant Physiol.* **2011**, *155*, 667–682.

(55) Ralph, J.; Lu, F. The DFRC method for lignin analysis. Part 6. A modified method to determine acetate regiochemistry on native and isolated lignins. *J. Agric. Food Chem.* **1998**, *46*, 4616–4619.

(56) Morreel, K.; Ralph, J.; Kim, H.; Lu, F. C.; Goeminne, G.; Ralph, S.; Messens, E.; Boerjan, W. Profiling of oligolignols reveals monolignol coupling conditions in lignifying poplar xylem. *Plant Physiol.* **2004**, *136*, 3537–3549.

(57) Tokimatsu, T.; Umezawa, T.; Shimada, M. Synthesis of four diastereomeric lignin carbohydrate complexes (LCC) model compounds composed of a  $\beta$ -O-4 lignin model linked to methyl  $\beta$ -D-glucose. *Holzforschung* **1996**, *50*, 156–160.

(58) Toikka, M.; Sipilä, J.; Teleman, A.; Brunow, G. Lignin–carbohydrate model compounds. Formation of lignin–methyl arabinoside and lignin–methyl galactoside benzyl ethers *via* quinone methide intermediates. *J. Chem. Soc., Perkin Trans. 1* **1998**, 3813–3818.

(59) Toikka, M.; Brunow, G. Lignin–carbohydrate model compounds. Reactivity of methyl 3-O-( $\alpha$ -L-arabinofuranosyl)- $\beta$ -D-xylopyranoside and methyl  $\beta$ -D-xylopyranoside towards a  $\beta$ -O-4-quinone methide. *J. Chem. Soc., Perkin Trans. 1* **1999**, 1877–1883.

(60) Li, K.; Helm, R. F. Synthesis and rearrangement reactions of ester-linked lignin–carbohydrate model compounds. *J. Agric. Food Chem.* **1995**, *43*, 2098–2103.

(61) Fujimoto, A.; Matsumoto, Y.; Chang, H.-m.; Meshitsuka, G. Quantitative evaluation of milling effects on lignin structure during the isolation process of milled wood lignin. *J. Wood Sci.* **2005**, *51*, 89–91.

(62) Košíková, B.; Joniak, D.; Kosáková, L. On the properties of benzyl ether bonds in the lignin–saccharidic complex isolated from spruce. *Holzforschung* **1979**, *33*, 11–14.

(63) Lawoko, M.; Henriksson, G.; Gellerstedt, G. Characterization of lignin–carbohydrate complexes from spruce sulfite pulps. *Holzforschung* **2006**, *60*, 162–165.